THERMODYNAMIC ANALYSIS AND SIMULATION OF A NEW COMBINED POWER AND REFRIGERATION CYCLE USING ARTIFICIAL NEURAL NETWORK

by

Seyyed Abdolreza FAZELI*, Hossein REZVANTALAB, and Farshad KOWSARY
Faculty of Mechanical Engineering, University of Tehran, Tehran, Islamic Republic of Iran

Original scientific paper
UDC: 621.565.6
DOI: 10.2298/TSCI101102009F

In this study, a new combined power and refrigeration cycle is proposed, which combines the Rankine and absorption refrigeration cycles. Using a binary ammonia-water mixture as the working fluid, this combined cycle produces both power and refrigeration output simultaneously by employing only one external heat source. In order to achieve the highest possible exergy efficiency, a secondary turbine is inserted to expand the hot weak solution leaving the boiler. Moreover, an artificial neural network is used to simulate the thermodynamic properties and the relationship between the input thermodynamic variables on the cycle performance. It is shown that turbine inlet pressure, as well as heat source and refrigeration temperatures have significant effects on the net power output, refrigeration output, and exergy efficiency of the combined cycle. In addition, the results of artificial neural network are in excellent agreement with the mathematical simulation and cover a wider range for evaluation of cycle performance.

Key words: *combined cycle, ammonia water, exergy efficiency, artificial neural network*

Introduction

In recent years, the world demand for energy has increased continuously. Moreover, pollution caused by the exhaust emissions from industrial equipments has become of primary importance. There are a large amount of waste heats being released into the environment, such as exhaust gas from turbines and engines, and waste heat from power plants as well as heat pump condensers, which lead to serious environmental pollution. Therefore, it is necessary to apply more efficient energy conversion processes in order to minimize the negative environmental impact of utilizing energy resources.

The introduction of combined cycles has been a crucial development for improving overall energy conversion efficiency of power plants. Another recent improvement in thermal power cycles is based on using mixed working fluids. The motivation for using binary mixtures is that they exhibit a boiling temperature that varies during the boiling process, and their em-

* Corresponding author; e-mail: abfazeli@ut.ac.ir

ployment as working fluids, thus allows maintenance of a more constant temperature difference between them and variable temperature heat sources, and consequently reduced exergy losses in the heat addition process. To take advantage of this feature, Kalina [1] proposed the use of ammonia-water mixtures as the working fluids in the bottoming cycle of a combined cycle power plant. Although Kalina is recognized for introducing the multi-component working fluid power cycle and for bringing it to its current state, Maloney *et al*. [2] studied an absorption-type power cycle using a mixture of ammonia and water as a working fluid in the early 1950s. Since then, considerable efforts have been made to employ the ammonia-water mixtures in various power cycle applications.

A topic of recent interest is the idea of combined power and cooling cycles that use an ammonia-water working fluid. The cited advantages of combined operation include a reduction in capital equipment by sharing of components, and also the possibility of improved resource utilization compared to separate power and cooling systems [3, 4]. A combined thermal power and refrigeration cycle was proposed by Goswami [5], and some further researches on the cycle performance were carried out [6-12]. It could provide power output as well as refrigeration and used an absorption condensation instead of the conventional condensation process. However, this cycle had a major shortcoming. As it employed the ammonia-rich vapor in the turbine to generate power, and then the turbine exhaust passed through a heat exchanger (cooler) transferring sensible heat to the chilled water, the refrigeration output was relatively small. In order to produce a larger cooling effect, the working fluid should go through a phase change in the cooler. Zheng *et al*. [13] proposed a combined power/cooling cycle utilizing Kalina's technology. The modification was such that the flash tank in Kalina cycle was replaced by a rectifier which could obtain a higher concentration ammonia-water vapor for refrigeration. Moreover, a condenser and an evaporator were inserted between the rectifier and the second absorber. Considerable power and refrigeration output could be achieved by these improvements. Liu *et al.* [14] proposed a novel combined power and refrigeration cycle using ammonia-water mixture as the working fluid. They introduced a splitting/absorption unit into the combined power and refrigeration system. In a similar work, Zhang *et al.* [15] proposed a new model, operating in a parallel combined cycle mode with an ammonia-water Rankine cycle and an ammonia refrigeration cycle, interconnected by absorption, separation, and heat transfer processes. The effects of the critical thermodynamic parameters on both energy and exergy efficiencies were investigated. More recently, another combined refrigeration and power system was suggested by Wang *et al.* [16] which combined Rankine and absorption refrigeration cycles.

However, it should be noted that determining thermodynamic properties of water ammonia mixtures, which have significant effect on the performance of cycles, and analyzing thermodynamic characteristics of the combined power and cooling cycles usually require a large amount of computer power and time. The former is presented in the literature as limited experimental data or complex differential equations [17-20] and the latter is too complex because of thermodynamic property equations of fluid couples involving the solution of complex differential equations.

Instead of solving complex equations and applying limited experimental data, faster and simpler solutions can be obtained using the artificial neural networks (ANN). ANN are able to learn the key information patterns within multidimensional information domain. This technique can be used in modeling of complex physical phenomena such as in thermal engineering. The use of ANN for simulating complex systems and predicting properties of fluid parts is increasingly becoming popular in the last decades. This is mostly because ANNs can be trained

just by using examples and they do not need an explicit formulation of physical relationships of concerned problem.

Different types of ANN have shown a good potential in solving complex engineering problems. The standard back propagation ANN techniques as well as several other common methods has been successfully adopted for analysis of different parameters in various mechanical systems like solar steam generating plant [21], refrigeration system [22], heat transfer [23], internal combustion engines [24], chemical systems [25], absorption chiller systems [26], fin-tube refrigerating heat exchangers [27], gas/solid sorption chilling machines [28], absorption chiller systems [29], *etc*. The back propagation ANN technique is a generalized approach, which has been derived from the Widrow error correction rule [30]. The original Widrow-Hoff technique utilized an error signal that was defined as the difference between the reference value and predicted output. Weights were changed in proportion to the error, which diminished the error in the direction of the gradient.

In this paper, a more advanced combined power and refrigeration cycle is proposed and examined, as an improvement upon the configuration analyzed by Hasan *et al.* [6], which was originally proposed by Goswami in 1995. This plant operated in a parallel combined cycle mode with an ammonia-water Rankine cycle and an ammonia refrigeration cycle, interconnected by absorption, separation, and heat transfer processes. The proposed cycle is shown schematically in fig. 1. Two major differences are detected between this proposed cycle and the one in [6]. Firstly, the rectified vapor leaving the superheater (state 8) is expanded to a mid pressure in the turbine, then fed to a condenser and throttled to the cycle low pressure before entering the refrigeration heat exchanger. This leads to an enhanced refrigeration output compared to relatively small load extracted from the cycle examined in [6]. Secondly, the stream entering the recovery heat exchanger earns heat using the external heat source. Consequently, the hot weak solution exiting the boiler is not cooled and throttled back into the absorber, but is combined with the rectified liquid (state 6) and fed into a second superheater. Thus, it can be expanded through another turbine, providing some extra output work. As a result of these modifications, employing the hot weak solution to produce more useful work and a condenser to achieve a higher refrigeration load can elevate the cycle's energy and exergy efficiencies to a more beneficial level.

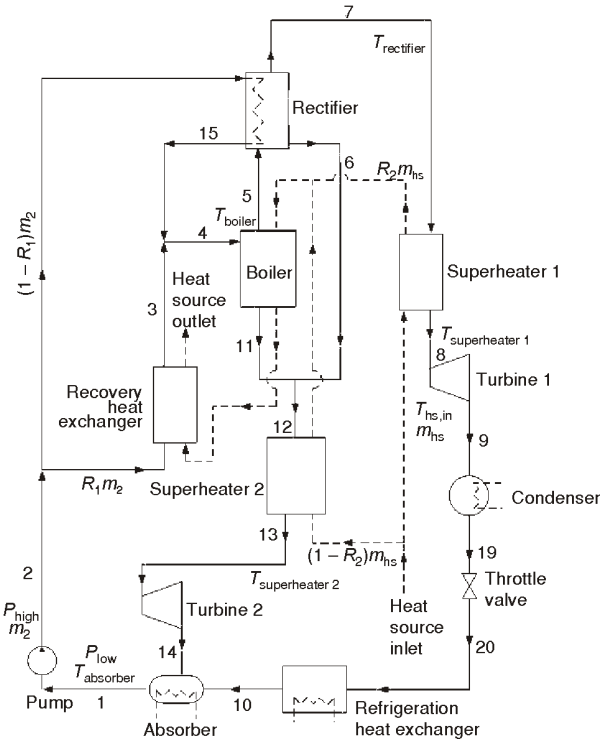

Figure 1. Schematic diagram of the combined power and refrigeration cycle

The main objective of the present work is to investigate the effect

of key thermodynamic parameters on the cycle performance. A neural network is created and trained in order to evaluate the cycle outputs in the whole acceptable range of pre-defined input parameters. The effect of different networks using various hidden layer neurons of the relative errors of estimating cycle parameters is also investigated.

Mathematical modeling and assumptions

The proposed cycle is a combination of Rankine cycle and absorption refrigeration cycle, which can produce both power and refrigeration simultaneously with only one heat source. The use of ammonia-water mixtures as the working fluid provides a significant reduction in heat transfer irreversibility in the boiler when used with a sensible heat source [6].

As shown in fig. 1, the basic concentration saturated solution which leaves the absorber is considered to be at the cycle low pressure P_{low} and at constant absorber temperature, assumed to be 300 K in the present study. The saturated liquid solution is then pumped to a high pressure (state 2). The high pressure liquid is split into two streams: one is directed towards the rectifier and the other passes through a recovery heat exchanger; where after recovering waste heat is mixed with the first stream leaving the rectifier and then enters the boiler (state 4). The mixture is partially boiled in the boiler, producing a vapor rich in ammonia and a hot, liquid weak solution. The vapor is condensed in the rectifier to increase the ammonia content of the vapor, until reaching a concentration of 1 kg of ammonia per kg of total mixture. at rectifier temperature (state 7). The rectified vapor is superheated and expanded through a turbine to a mid pressure P_{mid}, then fed to a condenser and throttled to the cycle low pressure before entering the refrigeration heat exchanger. The exit temperature from the throttle valve is lower than ambient temperature, allowing a considerable refrigeration (cooling) load to be extracted from the pure ammonia liquid in the refrigeration heat exchanger.

On the other hand, the hot weak solution leaving the boiler (state 11) is combined with the rectified saturated liquid (state 6) and fed into a second superheater. The mixture is subsequently expanded through another turbine to the cycle low pressure, enabling the extraction of some additional output work. Finally, the weak solution leaving the turbine is fed into the absorber, where it is combined with the high concentration ammonia mixture which has provided the refrigeration output. The solution is then condensed by rejection of heat until reaching the specified absorber temperature.

The heat exchanged in superheaters, boiler, and the recovery heat exchanger were supplied by employing an external heat source stream of air, with entrance temperature in the range of 500-600 K. In addition, the recovery heat exchanger mass flow rate ratio R_1 and the heat source mass flow rate ratio R_2 were considered to be equal to 0.5, since they don't have any influence on total energy balance of the relevant process. The pressure drops and heat losses in pipe lines and the work required by the pump were also neglected. The exit temperatures from both superheaters were assumed to be 50 °C lower than the heat source inlet temperature. Furthermore, the refrigeration temperature (state 10) was varied from 10 to 40 °C lower than the environment temperature. The main assumptions are reflected in tab. 1.

Artificial neural network modeling

An ANN tries to recognize an approximate pattern between inputs and their desired outputs by imitating the brain functions. Their ability of learning by examples makes the ANN

more flexible and powerful than the parametric approaches. Thus, ANN can be used to find patterns and detect trends that are too complex to be noticed by either humans or other computer techniques.

An ANN compromises interconnected groups of artificial neurons and their respective weight building blocks; the behavior of the network depends largely on the interaction between these building blocks which are used in training the network in order to perform a particular function. Each neuron accepts a weighted set of inputs and responds with an output or activation function, which can be hard limit threshold function, log-sigmoid function, or hyperbolic tangent function as stated in eqs. (1)-(3).

Hard limit: $$f(x) \quad \begin{matrix} 0 & x & 0 \\ 1 & x & 0 \end{matrix} \tag{1}$$

Log-sigmoid function: $$f(x) \quad \frac{1}{1 \quad e^{x}} \tag{2}$$

Hyperbolic tangent sigmoid: $$f(x) \quad \frac{e^{x} \quad e^{x}}{e^{x} \quad e^{x}} \tag{3}$$

A typical ANN consists of three layers, an input layer which takes the input variables from the problem, a hidden layer(s) made up of artificial neurons that transform the inputs, and an output layer that stores the results. ANN are trained to get specific target output from a particular input, using a suitable learning method; therefore, the error between the output of the network and the desired output should be minimized by modifying the weights and biases. Afterwards, this trained network can be applied to the simulated system to predict the system outputs for the inputs which have not been introduced to the network during the training phase.

The training rule used in the current study is the back-propagation training algorithm. This algorithm is a gradient descent algorithm, in which the network weights are changed along the negative of the gradient of the performance function. For feed-forward networks, performance functions are usually considered as the average squared error between the network and the target outputs. This method is called back-propagation because of the way in which the gradient is computed for non-linear multilayer networks. Recently, the basic algorithm has undergone some modifications that are based on other standard optimization techniques, such as conjugate gradient and Newton methods. Properly trained back-propagation networks can achieve reasonable answers when presented with inputs that they did not see. This property makes it possible to train a network on a predefined set of input/target pairs and get acceptable results without training the network on all possible input/output pairs.

To model the relationship between combined power and refrigeration cycle variables and the second law efficiency, a feed-forward neural network with three hidden layers is employed in the study.

Results and discussion

The parametric analysis is performed to evaluate the effects of three major parameters on the combined cycle performance: turbine inlet pressure, heat source inlet temperature, and the refrigeration temperature. When one specific parameter is studied, other parameters are kept constant. The values of the constant parameters and the range in which three substantial variables are altered are shown in tab. 1.

Table 1 . Conditions assigned to the cycle parameters

Environment temperature [K]	300
Cycle low pressure [bar]	1
Absorber outlet temperature [K]	300
Working mixture mass flow rate [kgs^{-1}]	10
Heat source mass flow rate [kgs^{-1}]	130
Recovery heat exchanger mass flow rate ratio R_1	0.5
Heat source mass flow rate ratio R_2	0.5
1st turbine isentropic efficiency [%]	80
2nd turbine isentropic efficiency [%]	85
Pump isentropic efficiency [%]	100
The range of heat source inlet temperature [K]	500-600
The range of refrigeration temperature [K]	260-290
The range of turbine inlet pressure [bar]	12-26

As mentioned previously, a feed-forward neural network with three hidden layers is employed in the study in order to model the cycle performance based on the above input variables.

In order to achieve accurate results while decreasing the calculation time as much as possible, several networks have been trained and their respective errors associated with exergy efficiency, training calculation time, and number of total iterations was compared. To find the most suitable network, the effects of number of neurons at each hidden layer on the mentioned parameters have been investigated. After normalizing the total number of iterations (α), the calculation time (β) and errors in estimating exergy efficiency of the cycle (γ), with their relevant reference values, the parameter S representing the deviation of each ANN can be defined as eq. (4):

$$S \quad \|\alpha\| \quad \|\beta\| \quad \|\gamma\| \tag{4}$$

Therefore, smaller values of S indicate higher quality of the neural network, that is higher precision and less calculation time. Several ANNs have been trained in order to investigate the influence of number of neurons in each layer on deviation parameter S. Figure 2 indicates how the variation of neurons quantity affects the quality of the created network for different values of second and third layer neuron numbers. As it can be observed, increasing the number of neurons in the first layer, while fixing the number of neurons on the other layers will result in a minimum point for deviation parameter S.

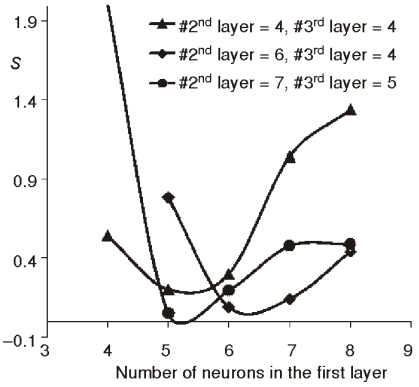

Figure 2. Effect of neuron number of the first hidden layer on network deviation

The same phenomenon is detected while increasing number of neurons in the third layer. As it can be seen in fig. 3, increasing the number of neurons in the third layer for fixed neuron values in the other layers results in a minimum point for deviation parameter S, thus an optimum network quality.

On the other hand, it was observed that raising the number of neurons in the second hidden layer causes a maximum for deviation parameter S, while no minimum point is observable. Figure 4 shows

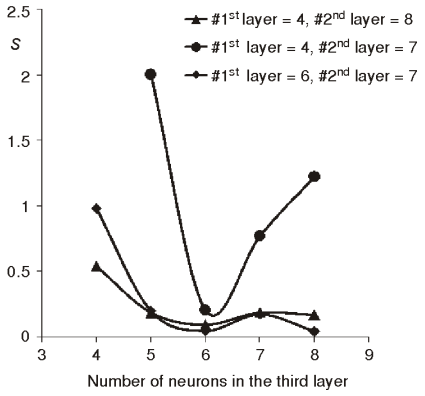

Figure 3. Effect of neuron number of the third hidden layer on ANN deviation

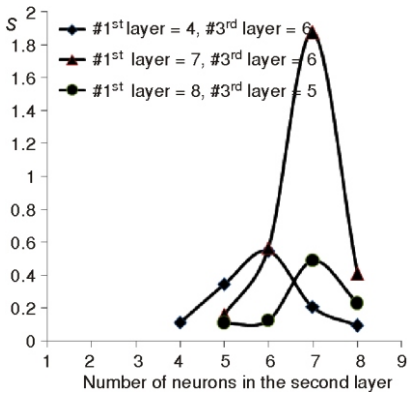

Figure 4. Effect of neuron number of the second hidden layer on ANN deviation

how the quality of the neural network becomes unfavorable for the second layer neuron numbers of about 6-7, in the examined range of neurons for other layers.

Considering the above effects, an exhaustive search method was applied to find the best values of neurons at each level which lead to the most fitting network. The result is shown in tab. 2.

Table 2. Normalized values of iteration number, calculation time, and efficiency error in different neuron numbers for three hidden layers of examined ANN

Number of neurons in the 1st layer	Number of neurons in the 2nd layer	Number of neurons in the 3rd layer	$\|\alpha\|$	$\|\beta\|$	$\|\gamma\|$	S
5	**8**	**8**	**0.01209**	**0.01105**	**0.01639**	**0.03953**
8	5	8	0.01209	0.0104	0.06253	0.08502
8	4	6	0.03747	0.02856	0.02025	0.08628
5	5	8	0.04351	0.03254	0.01317	0.08922
4	8	6	0.02055	0.01843	0.05337	0.09235
6	6	4	0.03948	0.02783	0.02812	0.09543
5	5	4	0.18171	0.15281	0.02495	0.35947
5	6	5	0.19782	0.16291	0.00793	0.36866
7	4	8	0.20548	0.16405	0.01047	0.38
5	4	8	0.20467	0.16744	0.00936	0.38147
7	8	6	0.21434	0.19065	0.00234	0.40734
5	7	7	0.21998	0.18488	0.007	0.41187
5	4	6	0.22039	0.20153	0.00866	0.43058

The first line in tab. 2 indicates the optimum choice of neuron numbers for training the neural network, in order to predict the cycle performance. As it can be noticed, the number of neurons in the first hidden layer should be lower than that of the second and third layers. This optimum network was employed to evaluate the cycle power as well as the refrigeration output and exergy efficiency in a wide range of working conditions, taking heat source inlet temperature, refrigeration temperature, and turbine inlet pressure as the input parameters.

For a turbine inlet pressure of 20 bar, heat source temperature of 500 K and refrigeration temperature difference of 40 °C with respect to the ambient, operating conditions obtained from the simulation are shown in tab. 3. The states indicated in the table correspond to locations given in the schematic of the cycle in fig. 1. It is obvious that the temperatures of states 8 and 13 which are defined by superheater temperatures are equal to T_{in}-50 and the refrigeration temperature (state 10) corresponds to T_0-40. The boiler and rectifier temperatures are also obtained using a slight variation in the conditions enforced by concentration and pressures of the absorber and boiling heat exchanger. Moreover, it can also be observed that a large fraction of the basic solution returns from the boiler to the absorber through the secondary superheater and turbine. In this case, only about 4% of the basic solution is directed from the rectifier towards the primary turbine and refrigeration heat exchanger as pure ammonia, enabling the extraction of power and refrigeration load. Therefore, the employment of the second turbine seems essential for making use of considerable amount of available exergy from the hot weak solution leaving the boiler.

Table 3. Operating conditions of the combined cycle at P_{high} = 20 bar, T_{in} = 500 K, T_{ref} = T_0-40

State	P [bar]	T [°C]	h [kJkg^{-1}]	s [kJkg^{-1}K^{-1}]	m [kgs^{-1}]	x
1	1	27	–149.926	0.257692	10	0.305169
2	20	27.1	–149.956	0.257692	5	0.305169
3	20	25.09275	3455.432	13.91454	5	0.305169
4	20	186.699	1777.74	4.788329	10	0.305169
5	20	140.7783	1729.192	5.196552	0.747389	0.834101
6	20	67.40514	123.2122	0.850858	0.343804	0.692775
7	20	67.40514	1353.064	4.254301	0.403585	1
8	20	177	1652.912	5.028429	0.403585	1
9	10.0729	117.0292	1524.774	5.028429	0.403585	1
10	1	–13	1262.923	5.308321	0.403585	1
11	20	140.7783	443.3603	1.756231	9.252611	0.262444
12	20	138.0287	431.8906	1.744269	9.596415	0.277861
13	20	177	2441.241	6.169578	9.596415	0.277861
14	1	89.3714	1938.908	6.169578	9.596415	0.277861
15	20	67.09759	100.0476	0.839203	5	0.305169
19	10.0729	24.99475	327.2191	1.115654	0.403585	1
20	1	–33.5172	327.2191	1.167804	0.403585	0.183751

Figure 5 shows the effect of turbine inlet pressure on net power output of the cycle. The curves correspond to a pressure range of 12-30 bar, and three different heat source temperatures, while refrigeration temperature is kept constant at T_{ref} = 260 K. It can be observed that in general, power output increases as the turbine inlet pressure is increased. This is due to the proven thermodynamic principle that the enthalpy drop across the turbine increases as the pressure ratio increases. It should be noted that the first turbine's exit pressure P_{mid} is only a function of condenser temperature, and thus remains constant as the high pressure is varied. Accordingly, increasing the inlet pressure of both turbines while outlet pressures are kept unchanged, results in an increased pressure ratio across both components; thereby increasing the net power output of the cycle. Moreover, it can be seen that the net power output increases with increasing heat source temperature. This is because a higher heat source temperature leads to a greater amount of heat exchanged in superheaters, and thereby a higher turbine inlet temperature and enthalpy. Increased enthalpy drop across both turbines then signifies a higher output work.

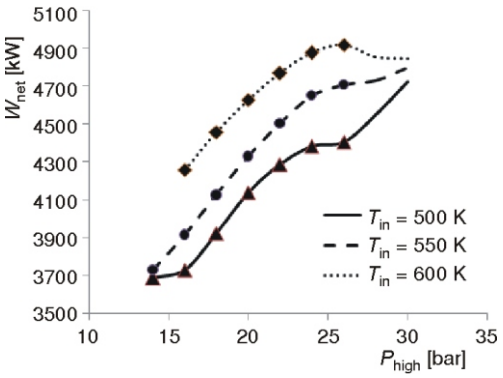

Figure 5. Effect of turbine inlet pressure on net power output for different heat source temperature

In all three curves, the values of net output work predicted by ANN show excellent agreement with the ones obtained from mathematical simulation, which are depicted by markers. In addition, for turbine inlet pressures higher than 26 bar, the mathematical modeling was unable to evaluate the cycle performance because of the limitations in calculating some of thermodynamic variables. However, the neural network can provide interesting solutions in this range of input parameters, which follow a reasonable trend based on previous values.

Figure 6 shows the effect of the turbine inlet pressure on the cycle refrigeration output for the same refrigeration temperature as the previous diagram. As it is observed, the refrigeration output tends to increase as the turbine inlet pressure is elevated. As the state of the working fluid exiting the refrigeration heat exchanger (point 10) is independent of the cycle's high pressure, the influence of this parameter on the state of the fluid entering the heat exchanger should be investigated. According to the previous discussion, raising the pressure ratio results in a higher enthalpy drop across the first turbine, hence a lower enthalpy and temperature at the turbine exit. Assuming that the working fluid experiences a pressure-constant process in condenser until reaching the saturated liquid condition, a decreased mid temperature is identical to a lower saturated liquid enthalpy for the pure ammonia exiting the condenser. Since the subsequent throttling process is assumed to be

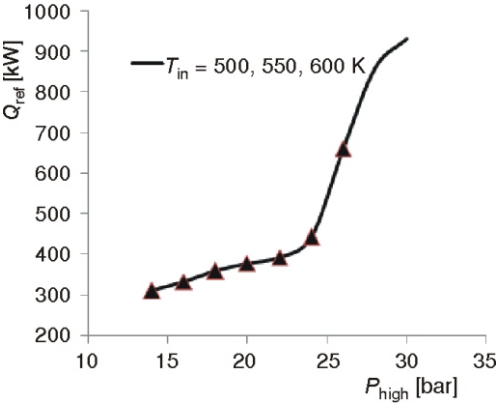

Figure 6. Effect of turbine inlet pressure on refrigeration output for different heat source temperature

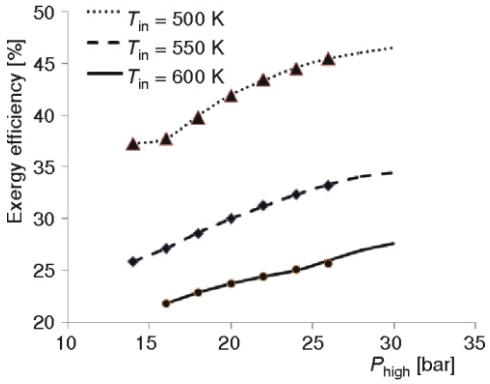

Figure 7. Effect of turbine inlet pressure on exergy efficiency for different heat source temperature

enthalpy-constant, an increased enthalpy drop occurs across the refrigeration heat exchanger, providing a higher refrigeration output.

It is also evident that the refrigeration output remains constant as the heat source temperature increases. This can be easily explained by considering that the inlet temperature of the refrigeration heat exchanger does not vary with the heat source temperature, and the outlet state is only a function of refrigeration temperature. Therefore, heat source inlet temperature has no influence on the refrigeration output.

Due to the cumulative effects of net power output and refrigeration output on the performance of the combined cycle, the exergy efficiency of the cycle increases by elevating the turbine inlet pressure, as shown in fig. 7. In other words, a higher total exergy, defined as maximum available work:

$$\psi = (h - h_0) - T_0(s - s_0) \tag{5}$$

is achieved due to the increased enthalpy at the heat source outlet, while the total input exergy supplied by the heat source remains constant.

On the other hand, combining the positive effect of increasing the heat source inlet temperature on the net power output of the cycle and its neutral impact on refrigeration output, it can be deduced that the total available exergy extracted from the cycle increases by raising the heat source inlet temperature. However, this increase is at the expense of a higher exergy input resulting from the raise in heat source temperature. The elevation in the required exergy input is more significant than the additional power output, thus resulting in lower exergy efficiency, as it can be deduced from fig. 7.

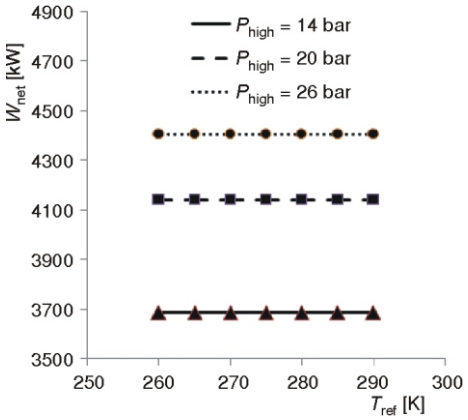

Figure 8. Effect of refrigeration temperature on net power output for different turbine inlet pressures

Figure 8 shows the effect of refrigeration temperature on the net power output at different turbine inlet pressures, when heat source inlet temperature is set to 500 K. It can be observed that the net power output remains constant as the refrigeration temperature increases. This is due to the fact that the variation of refrigeration temperature cannot change the turbines inlet and outlet conditions.

On the other hand, the refrigeration temperature directly affects the amount of cooling capacity since it alters the temperature and thus the enthalpy at refrigeration heat exchanger outlet. As it is indicated in fig. 9, cooling capacity of the cycle increases with refrigeration temperature in an approximately linear pattern, due to an increase in enthalpy rise across the heat exchanger.

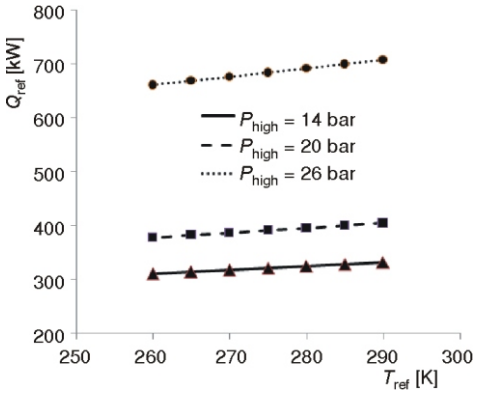

Figure 9. Effect of refrigeration temperature on cooling capacity for different turbine inlet pressures

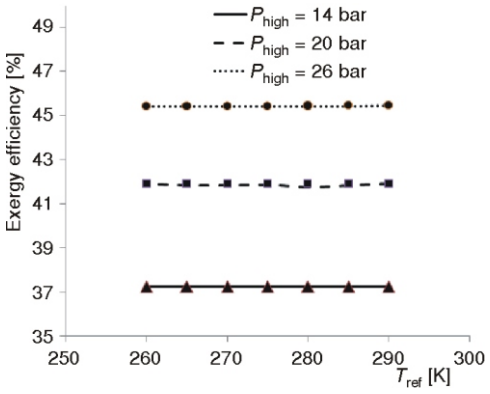

Figure 10. Effect of refrigeration temperature on exergy efficiency for different turbine inlet pressures

Finally, the variation of exergy efficiency with refrigeration temperature is shown in fig. 10. As it was expected from previous investigations, increasing the refrigeration temperature slightly increases the exergy efficiency of the cycle as a result of its combined neutral effect on net power and positive effect on refrigeration output. However, this change is relatively small due to the insignificant amount of increase in refrigeration output with respect to the total input exergy.

In addition, the results obtained for exergy efficiency of the cycle from the neural network are completely consistent with the data obtained from mathematical simulation. The maximum error associated with estimating the efficiency in the whole range of consideration was observed to be less than 0.07%.

Conclusions

A new combined power and refrigeration cycle using ammonia-water mixture as the working fluid is proposed, which employs two independent turbines and one cooling heat exchanger to produce both power and refrigeration output simultaneously, with only one heat source. Moreover, a feed-forward neural network with three hidden layers was used to simulate the thermodynamic properties of the working mixture and the relationship between the input thermodynamic parameters on the cycle performance.

Optimum values of neuron numbers in each of the hidden layers was identified to obtain an optimum network minimizing the number of required iterations, calculation time, and exergy efficiency estimating error. It was shown that temperature turbine inlet pressure, heat source temperature, and refrigeration temperature have significant effects on the net power output, refrigeration output, and exergy efficiency of the cycle. In addition, the insertion of the secondary turbine for expanding the hot weak solution leaving the boiler made it possible to achieve significant amounts of output work and cooling rates. The results predicted by the neural network are in excellent agreement with the ones obtained from mathematical simulation. The optimum ANN also provides reliable results in the range of input thermodynamic variables that the mathematical simulation fails to evaluate the cycle performance.

Nomenclature

h – enthalpy, [kJ^{-1}kg^{-1}]
m – mass flow rate, [kgs^{-1}]
P – pressure, [bar]
Q – heat load, [kW]
R_1 – recovery heat exchanger mass flow rate ratio, [–]
R_2 – heat source mass flow rate ratio, [–]
S – ANN deviation criteria, ($\|\alpha\|$ $\|\beta\|$ $\|\gamma\|$), [–]
s – entropy, [kJkg^{-1}K^{-1}]
T – temperature, [K]
W – power, [kW]
x – concentration of ammonia in water-ammonia mixture, [kgkg^{-1}]

Greek symbols

α – total number of iterations, [–]
β – calculation time for training the ANN, [s]
γ – error in estimating exergy efficiency of the cycle, [kJkg^{-1}K^{-1}]
ψ – stream exergy, [kJkg^{-1}]

Subscripts

hs – heat source
mid – middle
net – net value
ref – refrigeration outlet
0 – environment state

References

[1] Kalina, A. I., Combined Cycle and Waste-Heat Recovery Power Systems Based on a Novel Thermodynamic Energy Cycle Utilizing Low-Temperature Heat for Power Generation, ASME Paper, 83-JPGC-GT-3, 1983
[2] Maloney, J. D., Robertson, R. C., Thermodynamic Study of Ammonia-Water Heat Power Cycles, Oak Ridge National Laboratory Report, Oak Ridge, Tenn., USA., CF-53-8-43, 1953
[3] Erickson, D. C., Anand, G., Kyung, I., Heat-Activated Dual-Function Absorption Cycle, *ASHRAE Transactions, 110* (2004), 1, pp. 515-524
[4] Amano, Y., *et al*., A Hybrid Power Generation and Refrigeration Cycle with Ammonia-Water Mixture, *Proceedings,* Joint Power Generation Conference ASME, IJPGC2000-15058, 2000, pp. 1-6
[5] Xu, F., Goswami, D. Y., Bhagwat, S. S., A Combined Power/Cooling Cycle, *Energy, 25* (2000), 3, pp. 233-246
[6] Hasan, A. A., Goswami, G. Y., Vijayaraghavan, S., First and Second Law Analysis of Anew Power and Refrigeration Thermodynamic Cycle Using a Solar Heat Source, *Solar Energy, 73* (2002), 5, pp. 385-393
[7] Goswami, D. Y., *et al*., New and Emerging Developments in Solar Energy, *Solar Energy, 76* (2004), 1-3, pp. 33-43
[8] Tamm, G., *et al*., Theoretical and Experimental Investigation of an Ammonia-Water Power and Refrigeraton Thermodynamic Cycle, *Solar Energy, 76* (2004), 1-3, pp. 217-228
[9] Vidal, A., *et al*., Analysis of a Combined Power Andrefrigeration Cycle by the Exergy Method, *Energy, 31* (2006), 15, pp. 3401-3414
[10] Vijayaraghavan, S., Goswami, D. Y., A Combined Power and Cooling Cycle Modified to Improve Resource Utilization Efficiency Using a Distillation Stage, *Energy, 31* (2006), 8-9, pp. 1177-1196
[11] Martin, C., Goswami, D. Y., Effectiveness of Cooling Production with a Combined Power and Cooling Thermodynamic Cycle, *Applied Thermal Engineering, 26* (2006), 5-6, pp. 576-582
[12] Sadrameli, S. M., Goswami, D. Y., Optimum Operating Conditions for a Combined Power and Cooling Thermodynamic Cycle, *Applied Energy, 84* (2007), 3, pp. 254-265
[13] Zheng, D., *et al*., Thermodynamic Analysis of a Novel Absorption Power/Cooling Combined-Cycle, *Applied Energy, 83* (2006), 4, pp. 311-323
[14] Liu, M., Zhang, N., Proposal and Analysis of a Novel Ammonia-Water Cycle for Power and Refrigeration Cogeneration, *Energy, 32* (2007), 6, pp. 961-970
[15] Zhang, N., Lior, N., Development of a Novel Combined Absorption Cycle for Power Generation and Refrigeration, *ASME Journal of Energy Resources Technology, 129* (2007), 3, pp. 254-265
[16] Wang, J. F., Dai, Y. P., Gao, L., Parametric Analysis and Optimization for a Combined Power and Refrigeration Cycle, *Applied Energy, 85* (2008), 11, pp. 1071-1085
[17] Xu, F., Goswami, D. Y., Thermodynamic Properties of Ammonia-Water Mixtures for Power-Cycle Applications, *Energy, 24* (1999), 6,pp. 525-536

[18] Soleimani, A. G., Simple Equations for Predicting Entropy of Ammonia-Water Mixture, *International Journal of Engineering, 20* (2007), 1, pp. 97-106
[19] Patek, J., Klomfar, J., Simple Functions for Fast Calculations of Selected Thermodynamic Properties of the Ammonia-Water System, *International Journal of Refrigeration, 31* (1995), 4, pp. 228-234
[20] Thorin, E., Thermophysical Properties of Ammonia-Water Mixture for Prediction of Heat Transfer Areas in Power Cycles, *International Journal of Thermophysics, 22* (2001), 1, pp. 201-214
[21] Kalogirou, S. A., Applications of Artificial Neural-Networks for Energy Systems, *Applied Energy Journal, 67* (2000), 1-2, pp. 17-35
[22] Ertunc, H. M., Hosoz, M., Artificial Neural Network Analysis of a Refrigeration System with an Evaporative Condenser, *Appl. Therm. Eng., 26* (2006), 5-6, pp. 627-635
[23] Jambunathan, K., *et al.*, Evaluating Convective Heat Transfer Coefficients Using Neural Networks, *International Journal of Heat and Mass Transfer, 39* (1996), 11, pp. 2329-2332
[24] Parlak, A., *et al*., Application of Artificial Neural Network to Predict Specific Fuel Consumption and Exhaust Temperature for Adiesel Engine, *Appl. Therm. Eng., 26* (2006), 8-9, pp. 824-828
[25] Arcaklioglu, E., Performance Comparison of CfCs with Their Substitutes Using Artificial Neural Network, *Int. J. Energy Res., 28* (2004), 12, pp. 1113-1125
[26] Bechtler, H., *et al*., New Approach to Dynamic Modeling of Vapor-Compression Liquid Chillers: Artificial Neural Networks, *Applied Thermal Engineering, 21* (2001), 9, pp. 941-953
[27] Pacheco-Vega, A., *et al*., Neural Network Analysis of Fin-Tube Refrigerating Heat Exchanger with Limited Experimental Data, *International Journal of Heat and Mass Transfer, 44* (2001), 4, pp. 763-770
[28] Palau, A., Velo, E., Puigjaner, L., Use of Neural Networks and Expert Systems to Control a Gas/Solid Sorption Chilling Machine, *International Journal of Refrigeration, 22* (1999), 1, pp. 59-66
[29] Chow, T. T., *et al*., Global Optimization of Absorption Chiller System by Genetic Algorithm and Neural Network, *Energy Buildings, 34* (2002), 1, pp. 103-109
[30] Widrow, B., Hoff, M. E., Adaptive Switching Networks, in: Parallel Distributive Processing, Vol. 1, MIT Press, Cambridge, Mass., USA, 1986, pp. 318-362

Paper submitted: November 2, 2010
Paper revised: December 18, 2010
Paper accepted: December 23, 2010